

## **A Learned Reconstruction Network for bone SPECT Imaging**

**Mr. Afef Houimli**

*University of Tunis El Manar,  
Higher Institute of Medical Technologies of Tunis,  
Research Laboratory in Biophysics and Medical Technologies LR13ES07  
Tunis, 1006, Tunisia,  
Houimliafef13@gmail.com; Tel.: +21627103125*

### **Abstract**

Bone Single-Photon Emission Computed Tomography (SPECT) is a vital diagnostic tool for skeletal pathologies, yet it faces significant challenges including high Poisson noise, low spatial resolution, and time-consuming. This study proposes a novel reconstruction method based on Convolutional Neural Networks (CNN) to overcome these limitations. In this paper, we developed a novel reconstruction model. This model was trained using a diverse dataset comprising a clinical dataset of 31 bone SPECT examinations, a Shepp-Logan phantom, and a Jaszczak phantom. Quantitative evaluation was performed using Mean Square Error (MSE), Peak Signal-to-Noise Ratio (PSNR), Structural Similarity Index (MSSIM), and execution time. The proposed method (CNNR) was compared against iterative algorithms, specifically MLEM and OSEM. Results on both phantom and clinical data demonstrate that the proposed CNN-based method significantly outperforms iterative techniques. Quantitative analysis showed that the CNNR method achieved a higher PSNR (78.65) and a superior SSIM (0.987). Notably, the execution time was substantially reduced to 53.57 seconds per slice. Qualitative assessment confirmed that our method effectively preserves fine details, and lesion boundaries, while suppressing noise. The proposed method provides a high-quality, computationally efficient to iterative methods for bone SPECT imaging. Offering a significant potential for improving diagnostic accuracy in nuclear medicine.

**Keywords:** Bone SPECT, Image Reconstruction, Convolutional Neural Networks (CNN), Deep Learning.

### **1. Introduction**

Bone Single-Photon Emission Computed Tomography (SPECT) imaging is an essential diagnostic modality for identifying various skeletal pathologies, such as metastases and fractures. However, its performance is inherently limited by factors such as high statistical (Poisson) noise, low spatial resolution, and artifacts due to attenuation and scatter. Traditional iterative reconstruction methods, such as MLEM (Maximum Likelihood

Expectation Maximization)[1] and OSEM (Ordered Subset Expectation Maximization)[2-4], while effective in enhancing contrast and resolution, are often penalized by prolonged computation times (up to several minutes per slice) and struggle to preserve fine details while effectively suppressing noise, particularly in low-count bone SPECT examinations.

In response to these challenges, machine learning (ML) has emerged as a promising approach for improving image quality across various medical imaging modalities, including Magnetic Resonance Imaging (MRI)[5] , Computed Tomography (CT) [6] , Positron Emission Tomography (PET)[7] , and SPECT [8–10]. Several studies have demonstrated the ability of these techniques to generate high-quality images, characterized by a substantial reduction in noise and blurring artifacts. Among ML algorithms, Convolutional Neural Networks (CNNs), a category of deep learning algorithms, have revolutionized the field of computer vision. Inspired by the functioning of the visual cortex, CNNs excel at processing structured data such as images by automatically learning hierarchical features directly from raw data[11] . Their unique architecture enables them to detect complex patterns and perform tasks such as object classification, detection, and segmentation with remarkable accuracy. These capabilities make CNNs a particularly suitable tool for addressing the inherent limitations of bone SPECT image reconstruction.

In this paper, we present a new CNN-based reconstruction method specifically designed for bone SPECT imaging. The structure of this paper is as follows: Section 2 details the proposed method. The obtained results are presented and analyzed in Section 3. Finally, Section 4 concludes the study and proposes future research directions.

## 2. Materials and Methods

Reconstruction model:

### TRAINING DATA:

The proposed method was trained on two different SPECT phantoms: Shepp-Logan phantom and Jaszczak phantom, and a bone SPECT dataset containing 31 bone SPECT exams, 10 males and 21 females aged between 45 and 75, obtained from the nuclear medicine department of the National Oncology Institute “Salah AZAIZE” of TUNIS.

For each pixel 128\*128 projection, Sinograms were computed using the following equation:

$$S_i = \sum_{j=1}^{N*M} P_{ij} X_j \quad (1)$$

Where N is the number of projection angles, and M is the number of bin measurements per projection angle.

$S_i$  is the resulted sinogram at voxel j;  $X_j$  is voxel j at the projection .

$P_{ij}$  is the transfer matrix which presents the probability that a photon emitted from the voxel image j is detected in projection bin i.[12]

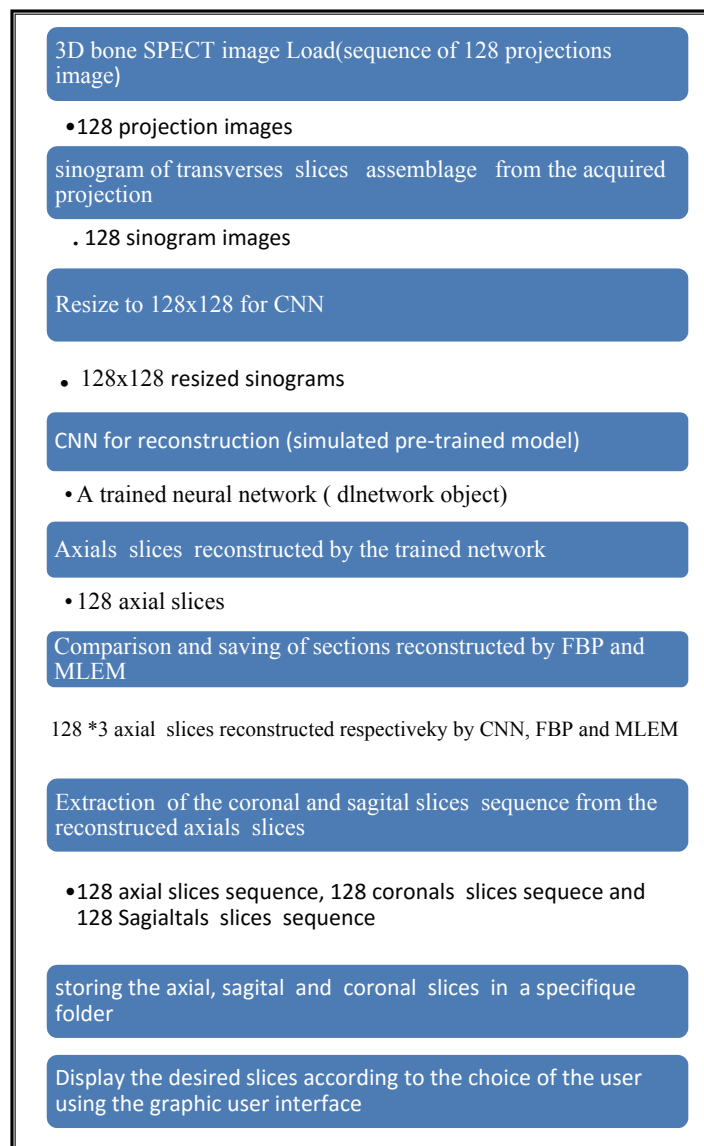
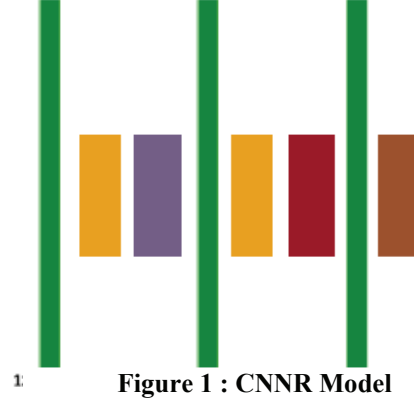


**Figure 1:** Proposed method

### Convolutional Neural Network

The proposed method based on a Convolutional Neural Network (CNN), a specialized subtype of deep feed-forward artificial neural networks. CNN's have been employed: to parse visual representations with many applications such as image classification and recognition [13], recommender systems [14] and medical image analysis [15]. The proposed CNN integrates convolutional, pooling, and fully connected layers. The pooling layers perform spatial subsampling by retaining dominant features, thereby reducing dimensionality and effectively preventing overfitting [16]. One key advantage of CNNs is their minimal preprocessing requirements and reduced dependence on expert prior knowledge, unlike traditional methods that demand extensive data manipulation and domain expertise [17].

The proposed CNN model for tomographic reconstruction consists of three sequential stages (Figure 1):



The model was trained with 31 bone SPECT exams, 90% for training and 10% for validation.

For a quantitative comparison, we computed for each patient the means CNR, means PSNR, means SSIM metrics and the means execution time of slices that contain the lesion.

Mean square error (MSE)

$$MSE = \frac{1}{AB} \sum_{i=1}^A \sum_{j=1}^B (C - D)^2 \quad (2)$$

Where C is the original slice and D is the reconstructed slice, A and B are the dimensions of these images

Peak Signal to Noise Ratio(PSNR) is defined as:

$$PSNR = 10 \log \frac{255^2}{MSE} \quad (3)$$

Structural Similarity (MSSIM) defined as:

$$MSSIM = \frac{1}{S} \sum_{k=1}^S \frac{(2 * a_i * a_j + c)(2 * \sigma_{ij} + c')}{(a_i^2 + a_j^2 + c) + (\sigma_i^2 + \sigma_j^2 + c')} \quad (4)$$

Where i and j presents respectively the original and the denoised slice;  $a_i$ ,  $a_j$ ,  $\sigma_i^2$  and  $\sigma_j^2$  denote the mean and the variance of the image and their estimation;  $\sigma_{ij}$  is the covariance of image i and j; c and c' are small constants to have usually a denominator different to zero and S is the total number of the local windows of the image.

### 3. Results and Discussion:

The sequence of Shepp-Logan projections was additionally randomized with a Medium Poisson noise level. The Poisson noise level was used by scaling the

sinogram value to 50%. Then, we applied the reconstruction methods to the noisy sequence. To present the phases introduced in Section 2, Fig. 3 outlines the axial slices resulted for the different methods.

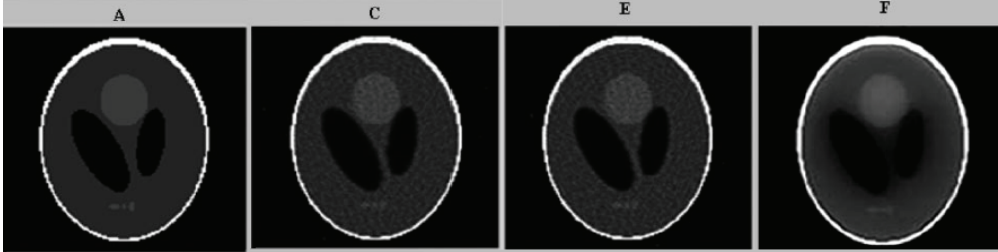


**Figure 3:** Axial slices of the tomographic Shepp-Logan Phantom (SLP) image reconstructed from noisy projections (projection 64) (A), using the following algorithms: 2D-MLEM (C), 2D-OSEM (E) and CNNR (E)

Figure 3 show that the proposed method (Figure. 3F) allows the preservation of the original structure during reconstruction by removing noise and conserving contrast and details. Whereas the iterative method used alone (Figure. 3C and 3E) attenuates the detail by giving a blur effect on the edges of the areas and making the extraction and the location of the edges difficult subsequently, the image form appeared slightly smooth and noisy.

Table1 resume the performance parameters for different reconstruction techniques.

**Table 1:** Performance parameters for reconstruction technique

Performance measures	MLEM	OSEM	Proposed method
MSE means	0,0056	0,00577	0,00577
PSNR means	70,798	70,696	78,646533
MSSIM means	2,1.10-5	2,1. .10-5	4,2. .10-5
Execution time(sec)	244,01995	78,96	53.570688

Quantitative analyses were used to evaluate the reconstruction methods. The optimum method has the lowest value of MSE and execution time and the highest value of PSNR and MSSIM. From Table 1, we note that the value of these metrics favored the proposed method which provides the highest value of

MSSIM (4,2.10-5) and PSNR (78,646533). This result demonstrates that the proposed method reconstructs a more similar structure than the other algorithms. Furthermore, the proposed method provides the lowest values of MSE (0,00577) and execution time (68.57) compared to other algorithms. This demonstrates that the proposed reconstruction algorithm preserves the edges and the quantitative information while removing noise. This method succeeds in keeping the compromise between noise reduction and details preservation. From this result, we can conclude

that the proposed method ensures an accurate reconstruction in lower computational time compared to other algorithm.

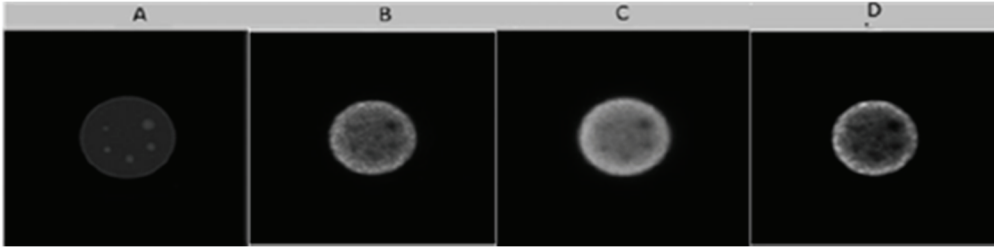


**Figure 4:** Axial slices (slice 73) reconstructed from the SPECT image of a Jaszczak phantom. (A) CT image; (B) Slice reconstructed by MLEM with 10 iterations; (C) Slice reconstructed by OSEM with (8 iterations and 4 subsets); (D) Slice reconstructed by CNNR.

From Figure 4, it can be seen that the shape of the sphere seems more spherical and the background less uniform in the reconstructed slice by CNNR method. Whereas in the reconstructed slice with the other methods, the shape of the sphere seems slightly smoothed and attenuated, making the extraction and localization of the contours difficult and giving a much noisier image. This result shows the accuracy and efficiency of our proposed method in the reconstruction. It allows better preservation of detail and region boundaries than the other methods.

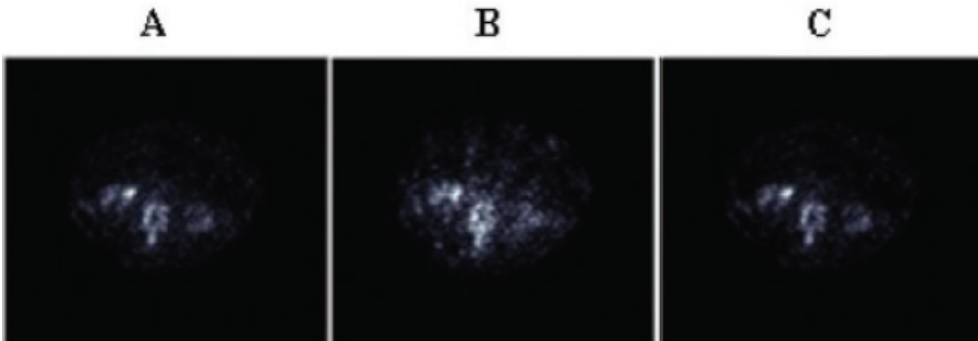


**Figure 5:** Axial slices of the clinical SPECT data, reconstructed by MLEM with 10 iterations; (C) Slice reconstructed by OSEM (8 iterations and 4 subsets); (D) Slice reconstructed by CNNR.

As shown in Figure 5, the CNNR method enhances the visibility of anomalies and fine details while reducing background artifacts and noise, preserving image contrast, regional boundaries, and singularities, and enabling more accurate lesion detection compared with the iterative method alone, which tends to attenuate details and hinder contour extraction.

## 5. Conclusion

In this paper, we presented a novel Convolutional Neural Network (CNN)-based reconstruction method for bone SPECT imaging. The proposed method was

rigorously tested on two distinct SPECT phantoms (Shepp-Logan and Jaszczak) and our dedicated bone SPECT database, demonstrating its accuracy and robustness in reconstruction. Our approach significantly improved image quality by reducing noise and preserving fine details, while also achieving a substantial reduction in computational time compared to traditional iterative methods. Summing up the results, it can be concluded that the proposed algorithm effectively enhances the quality of SPECT images in terms of noise reduction, accuracy, and reconstruction robustness. This work highlights the strong potential of deep learning to improve diagnostic accuracy and efficiency in nuclear medicine, paving the way for future advancements in medical image reconstruction.

## 5. Patents

**Funding:** This research received no external funding.

**Institutional Review Board Statement:** Not applicable.

**Informed Consent Statement:** Not applicable.

**Data Availability Statement:** Data are contained within the article

**Conflicts of Interest:** The authors declare no conflicts of interest.

## Abbreviations

The following abbreviations are used in this manuscript:

SPECT Single-Photon Emission Computed Tomography

OSEM Ordered Subset Expectation Maximization

MLEM Maximum Likelihood Expectation Maximization

CNN Convolutional Neural Networks

MSSIM Structural Similarity Index

ML machine learning

MRI Magnetic Resonance Imaging

CT Computed Tomography

PET Positron Emission Tomography

## References

[1] Bruyant, P. P.; Analytic and iterative reconstruction algorithms in SPECT. *J. Nucl. Med* **2002**, *43*(10), 1343-1358.

[2] Hudson, H.M.; Larkin, R. S. Accelerated image reconstruction using ordered subsets of projection data. *IEEE Trans. Med. Imaging* **1994**, *13*(4), 601–609. DOI 10.1109/42.363108.

[3] Blocklet, D.; Seret, A.; Popa, N.; Schoutens, A. A maximum likelihood reconstruction with ordered subsets in bone SPECT. *J. Nucl. Med* **1999**, *40*(12), 1978–1984. PMID 10616874.

[4] Lalush, D.; Tsui, B. M. W. Performance of ordered-subset reconstruction algorithms under conditions of extreme attenuate on and truncation in myocardial SPECT. *J. Nucl. Med* **2000**, *41*(4), 737–744. DOI 10.1.1.124.8728.

- [5] Yang, G.; Simiao, Y.; Hao, D.; Greg, S.; Pier, L. D. DAGAN: Deep de-aliasing generative adversarial networks for fast compressed sensing MRI reconstruction. *IEEE Trans. Med. Imaging* 2018, 37(6), 1310–1321.
- [6] DOI 10.1109/TMI.2017.2785879.
- [7] Gupta, H.; Jin, K. H.; Nguyen, H. Q.; McCann, M. T.; Unser, M. CNN based projected gradient descent for consistent CT image reconstruction. *IEEE Trans. Med. Imaging* 2018, 37(6), 1440–1453. DOI 10.1109/TMI.2018.2832656.
- [8] Hwang, D.; Kang, S. K.; Kim, K. Y.; Seo, S.; Paeng, J. C. Generation of PET attenuation map for whole-body time-of-flight 18F-FDG PET/MRI using deep neural network trained with simultaneously reconstructed activity and attenuation maps. *J. Nucl. Med* 2019, 60(8), 1183–1189. DOI 10.2967/jnumed.118.219493.
- [9] Charalambos, Ch.; Loizos, K.; Christos, L.; Costas, N. P. SPECT imaging reconstruction method based on deep convolutional neural network. IEEE Nuclear Science Symposium and Medical Imaging Conference (NSS/MIC), Manchester, UK., 26 October 2019 - 02 November 2019 ,
- [10] Dietze, M. M. A.; Branderhorst, W.; Kunnen, B.; Viergever, M. A.; De Jong, H. W. A. M. Accelerated SPECT image reconstruction with FBP and an image enhancement convolutional neural network. *EJNMMI Phys* 2019, 6(14), 1–12. DOI 10.1186/s40658-019-0252-0.
- [11] Wenyi, S.; Martin, G. P.; Yong, D. A learned reconstruction network for SPECT imaging. *IEEE Trans. Radiat. Plasma Med. Sci* 2021, 5(1), 26–34. DOI 10.1109/trpms.2020.2994041.
- [12] Liu L.; Ouyang W.; Wang X. A Survey of Convolutional Neural Networks: Analysis, Applications, and Prospects. *IEEE Trans. Neural Netw. Learn. Syst* 2022, (99):1-21.
- [13] Krizhevsky, A.; Sutskever, I.; Hinton, G. E. ImageNet Classification with Deep Convolutional Neural Networks. NIPS'12: Proceedings of the 26th International Conference on Neural Information Processing Systems , Lake Tahoe Nevada, United States, 03 December 2012.
- [14] Maroofa, Y.; Shailendra, N. Singh Image Recognition and Classification using CNN: A Review. International Conference on Electrical Electronics and Computing Technologies (ICEECT), Greater Noida, India, 29-31 August 2024.
- [15] Naveen K. N.; CVPR P. Hybrid Recommender System Using CNNs, Bi-Directional RNNs, and Autoencoders. *Communications on Applied Nonlinear Analysis* 2024, 31(7), 117-137.
- [16] Muhammad A. R. I.; Ali S. H.; Hybrid CNN-based Recommendation System. *Baghdad Science Journal* 2024, 21(2): 0592-0599.
- [17] Akbar S.; Peikari M.; Salama S.; Nofech-Mozes S.; Martel A. L. The transition module: a method for preventing overfitting in convolutional neural networks. *Computer Methods in Biomechanics and Biomedical Engineering: Imaging & Visualization* 2018. 7(3):260–265.
- [18] Tajbakhsh, N.; Y. Shin, J.; Suryakanth, R. G.; Todd Hurst, R.; Christopher, B. K.; Gotway, M. B., Convolutional Neural Networks for Medical Image Analysis: Full Training or Fine Tuning. *IEEE Transactions on Medical Imaging* 2016, 35(5) , 1299 – 1312.